

## VEHICLE DETECTION AND CLASSIFICATION FROM HIGH RESOLUTION SATELLITE IMAGES

Commission VI, WG VI/4

**KEY WORDS:** Region of Interest, Satellite Imaging Corporation, Bright vehicles, Otsu's threshold, SPOT-5, Connected Component Labeling, Cars, Trucks.

### ABSTRACT:

In the past decades satellite imagery has been used successfully for weather forecasting, geographical and geological applications. Low resolution satellite images are sufficient for these sorts of applications. But the technological developments in the field of satellite imaging provide high resolution sensors which expands its field of application. Thus the High Resolution Satellite Imagery (HRSI) proved to be a suitable alternative to aerial photogrammetric data to provide a new data source for object detection. Since the traffic rates in developing countries are enormously increasing, vehicle detection from satellite data will be a better choice for automating such systems. In this work, a novel technique for vehicle detection from the images obtained from high resolution sensors is proposed. Though we are using high resolution images, vehicles are seen only as tiny spots, difficult to distinguish from the background. But we are able to obtain a detection rate not less than 0.9. Thereafter we classify the detected vehicles into cars and trucks and find the count of them.

### 1. INTRODUCTION

Efforts to extract information from imagery have been in place ever since the first photographic images were acquired. Low resolution satellite images such as that obtained from LANDSAT, MODIS and AVHRR sensors provide only a vague idea about the scenes and will not provide any information about the objects found in the scene. Images obtained from these types of sensors can be used only for weather forecasting or meteorological applications. For feature extraction and object detection problems high resolution images is a basic requirement. High resolution sensors like CARTOSAT, IKONOS, QuickBird and SPOT provide detailed information about the objects as that of aerial images. The panchromatic band of QuickBird images reaches up to 60cm resolution which is as good as aerial images.

Though the availability of high resolution satellite images accelerate the process of object detection and automate such applications, vehicle detection from satellite images are still a challenging task. This is because, even in high spatial resolution imagery, vehicles are seen as minute spots which are unidentifiable from the foreground regions to detect. Classifying the detected vehicles is more serious as it is sometimes unable to distinguish large and small vehicles using naked eye itself even from high resolution images. Seeing the reference images in our work, this problem is clearly identified.

Earlier many researches have been performed on vehicle detection in aerial imagery [1, 2, 3] and later on the work is extended for satellite imagery. But the methods used for aerial imagery can't be directly applied for satellite images since vehicles are more vivid in aerial images. Most of the works

include morphological transformations for the classification of pixels into vehicle and non-vehicle targets [4, 5, 6]. Recent works in this area includes adaptive boosting classification technique [7] and an area correlation method [8] to detect vehicles from satellite images in which very good accuracy is achieved but the classification stage is not included. The most recent work in this field is by Zheng,Z. [9] where the quality percentage reaches 92%, but with aerial images of very high resolution having 0.15m.

The specialty of our work is, vehicles are detected even from satellite images of 2.5m resolution with acceptable accuracy. Both bright and dark vehicles are detected using the proposed method and then it is classified as cars and trucks. Results presented in the work reveals that the detection percentage reaches 90% irrespective of the poor quality of vehicles in satellite images.

### 2. METHODOLOGY

The method for vehicle detection consists of four steps: First, region of interest having roadways alone is extracted from the broad area image. Next, for the segmentation process, multiple thresholding which depends on the statistical properties of the image is chosen for finding bright vehicles. Detecting dark vehicles from the extracted segment is the third stage. Classification of vehicles and finding their count are the final stage of the automated approach. The algorithms developed were implemented, tested and analyzed using MATLAB™ software. The test images are obtained from Satellite Imaging Corporation, Texas, USA which is the official Value Added

Reseller (VAR) of imaging and geospatial data products. The simplified block diagram of the system is shown in fig. 1.

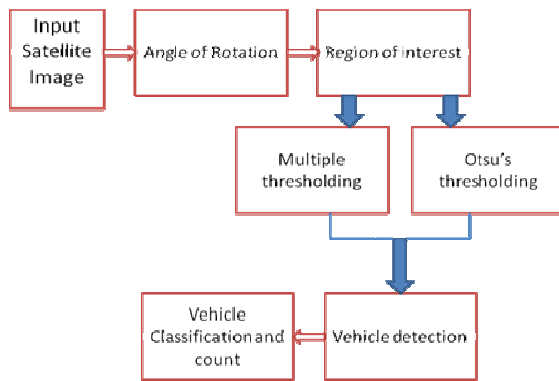


Figure 1: Overall Flow of the System

## 2.1 Region of Interest (ROI) Extraction

Most of the road segments may not be straight in the concerned satellite image. Therefore, before going directly to the region of interest segmentation we have to rotate the image in such a way that the road segment should be  $0^{\circ}$  with respect to the horizontal plane. After that selection of desired region of interest is done. The procedure is as follows:

### (i) Rotating the image

- (a) Enter the angle of rotation.  
if we are rotating it in the clockwise direction, the angle of rotation is negative and for anti-clockwise direction it will be positive.
- (b) Convert the value from cell string to string.
- (c) Convert the value from string to numeric.
- (d) Display the rotated image.

### (ii) Selecting the co-ordinates of the ROI

- (a) Select the (x,y) coordinates of the upper left corner point of the ROI.
- (b) Select the (x,y) coordinates of the lower right corner point of the ROI.
- (c) Merge the array x and y.
- (d) Convert the values from numeric to string.
- (e) Display the selected ROI co-ordinates.

### (iii) Region of interest Extraction

- (a) Subtract x co-ordinates to find width
- (b) Subtract y co-ordinates to find height
- (c) Crop ROI
- (d) Display the ROI

The figure shown below (fig.2) is a SPOT-5 panchromatic image of 2.5m resolution which is a highway in Oklahoma City.



Figure 2: SPOT-5 Panchromatic Image (2.5m)

As the road segment seen in the image is parallel to the horizontal plane, the angle of rotation is taken as  $0^{\circ}$ . The upper left and lower right corners of the ROI selected are shown in fig.3. The (x,y) co-ordinates of the selected region is given in fig.4. After finding the width and height of the region, the ROI is displayed in fig. 5.



Figure 3: Selecting the Coordinates of the Image

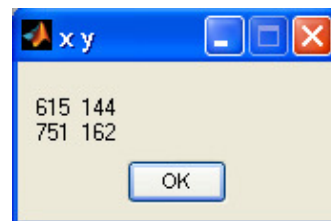


Figure 4: Displaying the Coordinates of the Image

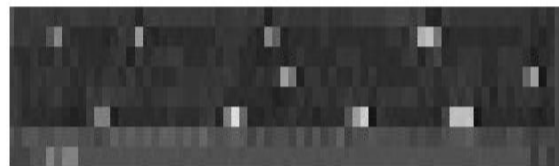


Figure 5: Region of Interest for Vehicle Detection

## 2.2 Multiple Thresholding for finding Bright Vehicles

Most of the cases, the intensity values of bright vehicles are greater than the intensities of the background. But some objects or regions on roads, such as lane markers and road dividers may have similar intensity values as that of bright vehicles. Also, each bright vehicle may not have same range of intensity because of the images taken at different times due to sun elevation and azimuth angles and sensor angles. Therefore, to identify only the vehicles and to avoid the detection of irrelevant objects, three different thresholds  $T_1$ ,  $T_2$ , and  $T_3$  are used. If  $M_1$  is a two dimensional matrix of image intensities, the procedure for finding the three threshold values is given below (fig.6):

$M_2$  is calculated by using  $M_1$   
 $M_2$ : for each row  $i$  in  $M_1$   
 $M_2[i] = \text{maximum\_intensity}[M_1, i]$   
 $T_1, T_2$  and  $T_3$  are calculated by using  $M_2$   
 $T_1: T_1 = \text{Mean}[M_2]$   
 $T_2: T_2 = \text{Minimum}[M_2]$   
 $T_3: T_3 = \text{Mean}[T_1, T_2]$

Figure 6: Finding Threshold Values

The concept is based on the fact that on a highway, bright vehicles have maximum intensity levels than any other objects. Therefore we are considering the maximum intensity in each row of  $M_2$  to calculate the three thresholds  $T_1, T_2$  and  $T_3$ . Thresholds  $T_1, T_2$ , and  $T_3$  are used to convert the test image to three different binary images Image-1, Image-2 and Image-3. Fig.7 shows the three thresholded images for calculated threshold values of 200, 149 and 175 for  $T_1, T_2$  and  $T_3$  respectively.

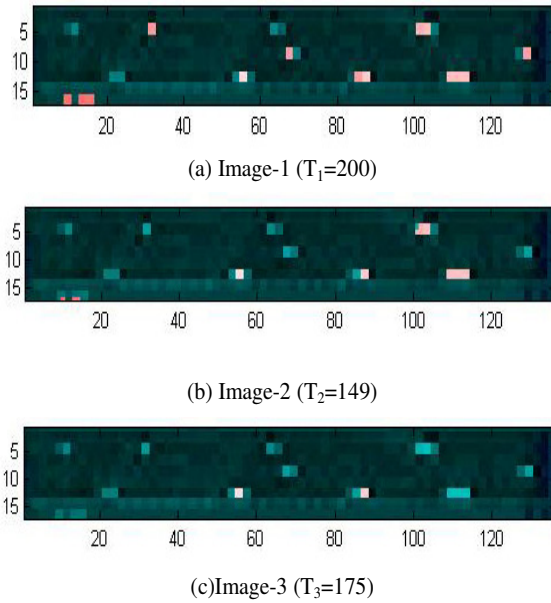


Figure 7: Thresholded Images

From fig.7, it is understood that many irrelevant objects are included in the thresholded images. Also some vehicles are common in the resultant images. In order to remove the irrelevant objects and to extract the common objects, the logical AND operation is performed among the binary images as given in eqn. (1), (2) and (3). The new binary images are shown in fig.8.

- New Image-1 = bitwise AND [Image-1, Image-2] (1)  
 New Image-2 = bitwise AND [Image-1, Image-3] (2)  
 New Image-3 = bitwise AND [Image-2, Image-3] (3)

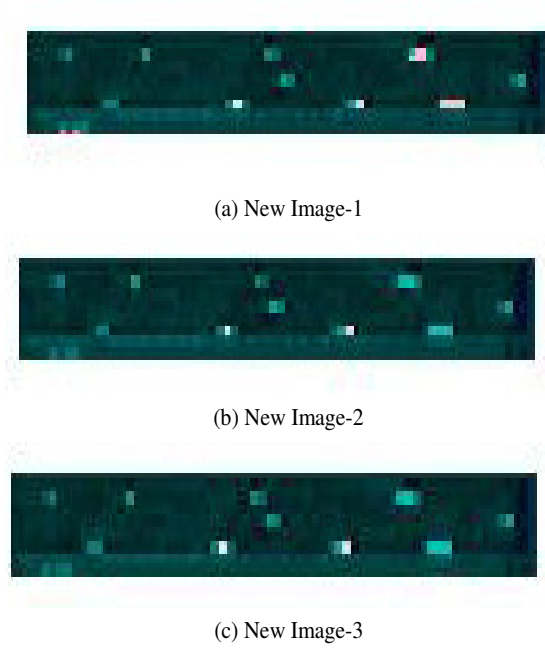


Figure 8: New Segmented Images

The final bright vehicle detected image (fig.9) is obtained as the logical OR operation performed among the new images (eqn.4).

$$\text{Final Bright Vehicle Image} = \text{bitwise OR} [\text{New Image-1}, \text{New Image-2}, \text{New Image-3}] \quad (4)$$



Figure 9: Bright Vehicle Detected Image

### 2.3 Otsu's Thresholding for finding Dark Vehicles

For the detection of dark vehicles, the Otsu's threshold [10] is used. Before applying the Otsu Threshold, a sliding neighborhood operation is applied to the test image [11]. In this method a 3-by-3 neighborhood of each and every pixel is selected. The nearby pixel is replaced by the minimum intensity value of this 3x3 window. The result is a darker pixel compared to the earlier one. This operation is followed by Otsu's thresholding to get the resultant dark vehicle detected image. The method check all pixel values in the image using equations 5 and 6 to find out which one is best to classify foreground and background regions, so that foreground regions are clearly distinguished from the scene depending on the quality of the image.

$$\text{Within Class Variance } \sigma_w^2 = W_b \sigma_b^2 + W_f \sigma_f^2 \quad (5)$$

$$\begin{aligned} \text{Between Class Variance } \sigma_B^2 &= \sigma^2 - \sigma_w^2 \\ &= W_b(\mu_b - \mu)^2 + W_f(\mu_f - \mu)^2 \quad (\text{where } \mu = W_b \mu_b + W_f \mu_f) \\ &= W_b W_f (\mu_b - \mu_f)^2 \end{aligned} \quad (6)$$

where weight, mean and variance of the image are represented by  $w$ ,  $\mu$  and  $\sigma^2$ . The foreground and background regions are represented as  $f$  and  $b$ . The detected dark vehicles are shown in fig.10.

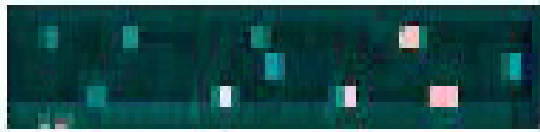


Figure 10: Dark Vehicle Detected Image

To avoid considering shadow of vehicles as dark vehicles, the bright and dark vehicle detected images are added using a logical OR operation (eqn. 7). This results in combining bright vehicles and their shadows together. The final vehicle detected image is shown in fig. 11.

Vehicle Detected Image = bitwise OR [Bright Vehicle Detected Image, Otsu's Thresholded Image] (7)



Figure 11: Resultant Vehicle Detected Image

#### 2.4 Vehicle Classification & Count

Before moving directly to the vehicle classification stage, a morphological dilation operation is performed as some vehicles may get splitted into parts after segmentation operation. Dilation will combine these parts into a single vehicle, which increase the detection accuracy of our vehicle detection algorithm. The structuring element used for the process is defined as eqn. (8):

$$SE = \begin{bmatrix} 1 & 1 & 1 \\ 1 & 1 & 1 \\ 1 & 1 & 1 \end{bmatrix} \quad (8)$$

From the detected vehicles, some of the parameters which are able to classify them as cars and trucks are calculated. In our work, width, height, and area of the detected vehicles are considered for the classification stage. For that connected component labeling is performed on the dilated image. First taking into account of all the connected components in the reference image, the average of each of these parameters is computed. Then, the three parameters for each and every detected vehicle are compared with the average values. If width, height, and area of the vehicle is greater than the average values it is considered as a truck, or else it is a car. The algorithm is given below:

- 1) Dilate Vehicle Detected Image using structuring element SE.
- 2) Perform Connected Component Labeling using 4-connected neighborhood.

- 3) Compute area, major axis (width) and minor axis (height) of labeled regions.
- 4) Obtain mean of these parameters.
- 5) Check whether area greater than mean area and Major axis length greater than mean major axis length and Minor axis length greater than mean minor axis length.
  - Yes – Increment truck count by 1
  - No – Increment car count by 1
- 6) Conversion from numeric to string for car and truck count.
- 7) Display the count in the message box.

The following figures (fig.12) show the car and truck counts for the vehicle detected image.



Figure 12: Car & Truck Counts of the ROI in the Reference Image

### 3. EXPERIMENTAL RESULTS

The results obtained for other two IKONOS (1m) and SPOT-5 (2.5m) images of highways in San Jose, CA and Barcelona, Spain are given below. The ROI for IKONOS image is with an angle of rotation of  $+13^{\circ}$  and for SPOT-5 image is with an angle of rotation of  $-10^{\circ}$ . To measure the performance of the algorithm, the results obtained are compared with the manual count of the vehicles; this is, by visually inspecting the region under study. The inferred results are given in table 1. For all the reference images, it is seen that, though the cars and trucks are not vivid even in the actual image, the results show that the detection rate is more than 90%.

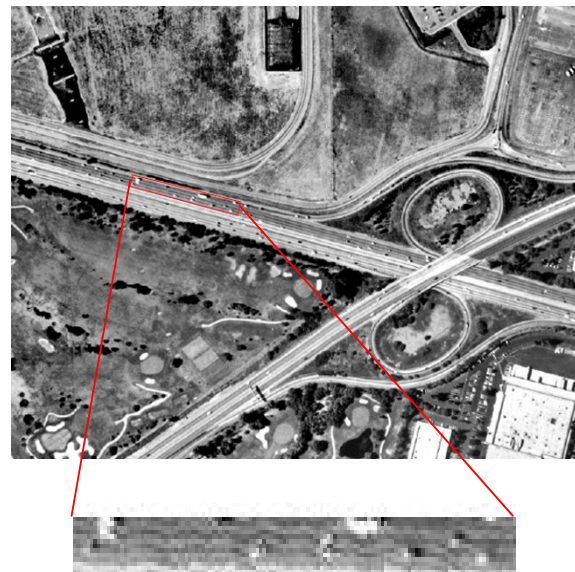


Figure13: IKONOS Panchromatic Image (1m) & ROI

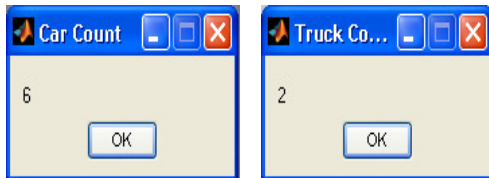


Figure 14: Car & Truck Counts of the ROI

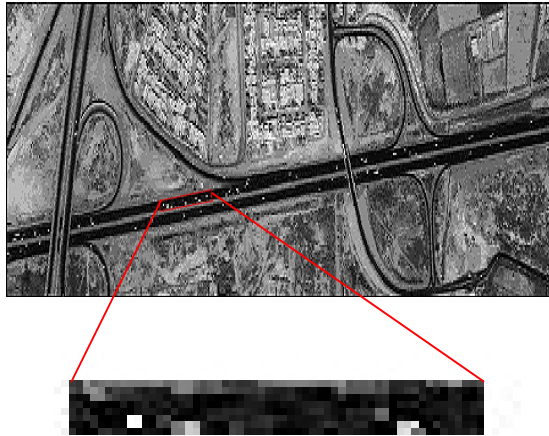


Figure 15: SPOT-5 Panchromatic Image (2.5m) & ROI

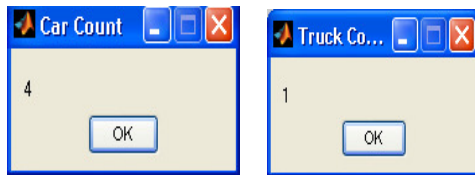


Figure 16: Car & Truck Counts of the ROI

Reference Images	Cars		Trucks		Total		
	Automatic Count	Manual Count	Automatic Count	Manual Count	Automatic Count	Manual Count	Detection Rate
Fig. 2 (2.5m resolution)	6	7	3	3	9	10	0.9
Fig. 13 (1m resolution)	6	6	2	2	8	8	1
Fig. 15 (2.5m resolution)	4	4	1	1	5	5	1

Table 1. Performance Evaluation

#### 4. CONCLUSION

In this paper, a multistep algorithm is designed for detecting vehicles from satellite images of different resolutions. The method also classifies and counts the number cars and trucks in the image. The proposed method is able to detect exact number of cars and trucks even from satellite images lower than 1m resolution in which vehicles are identified as some noisy white spots. But roads having high density traffic, there may be chances for increased error percentage since vehicles are very much closer in those cases. Availability of very high resolution hyper spectral data will make evolutionary changes in the field of feature extraction and can be used as a source to rectify

above mentioned problems. Further research should focus on these areas and experiment with maximum resources available to extract even the minute details from satellite images.

#### REFERENCES

Hinz, S., "Detection of vehicles and vehicle queues for road monitoring using high resolution aerial images", *Proceedings of 9th World Multiconference on Systemics, Cybernetics and Informatics*, Orlando, Florida, USA, pp.1-4, 10-13 July, 2005.

Schlosser, C., Reitberger, J. and Hinz, S., "Automatic car detection in high resolution urban scenes based on an adaptive 3D-model", *Proceedings of the ISPRS Joint Workshop on Remote Sensing and Data Fusion over Urban Areas*, Berlin, Germany, pp. 167-171, 2003.

Zhao, T., and Nevatia, R., "Car detection in low resolution aerial images", *Proceedings of the IEEE International Conference on Computer Vision*, Vancouver, Canada, pp. 710-717, 09-10 July, 2001.

Jin, X., and Davis, C.H., "Vehicle detection from high resolution satellite imagery using morphological shared-weight neural networks", *International Journal of Image and Vision Computing*, vol.25, no.9, pp.1422-1431, 2007.

Zheng, H., and Li, L., "An artificial immune approach for vehicle detection from high resolution space imagery", *International Journal of Computer Science and Network Security*, Vol.7, no.2, pp.67-72, 2007.

Zheng, H., Pan, L. and Li, L., "A morphological neural network approach for vehicle detection from high resolution satellite imagery", *Lecture Notes in Computer Science* (I. King, J. Wang, L. Chan, and D.L. Wang, editors), Vol. 4233, Springer, pp. 99-106. 2006.

Leitloff, J., Hinz, S., and Stilla, U., "Vehicle Detection in Very High Resolution Satellite Images of City Areas", *IEEE Trans. on Geoscience and Remote Sensing*, vol.48, no.7, pp.2795-2806, 2010.

Liu, W., Yamazaki, F., Vu, T. T., "Automated Vehicle Extraction and Speed Determination From QuickBird Satellite Images", *IEEE Journal of Selected Topics in Appl. Earth Observations and Remote Sensing*, vol.4, no.1, pp.1-8, 2011.

Zheng,Z., Zhou,G., Wang,Y., Liu,Y., Li,X., Wang,X. and Jiang,L., "A Novel Vehicle Detection Method With High Resolution Highway Aerial Image", *IEEE Journal of Selected Topics in Appl. Earth Observations and Remote Sensing*, vol.6, no.6, pp.2338-2343, 2013.

Otsu, N., "A threshold selection method from graylevel histograms," *IEEE Transactions. on Sys. Man Cyber.*, vol. 9, no. 1, pp. 62-66, 1979.

Aurdal, L, Eikvil, L., Koren, H., Hanssen, J.U., Johansen, K. and Holden, M. *Road Traffic Snapshot*, Report -1015, Norwegian Computing Center, Oslo, Norway. 2007.